

Article

Not peer-reviewed version

---

# From Functional Food to Therapeutic Prospect: Mechanistic Study of Gypenoside XVII in HeLa Cells

---

Sayed Sajid Hussain , Muhammad Maisam , [Shoaib Younas](#) , [Feng Wang](#) <sup>\*</sup> , [Weijie Li](#) <sup>\*</sup>

Posted Date: 11 December 2025

doi: 10.20944/preprints202512.1068.v1

Keywords: Gypenoside XVII; Hela; cell cycle analysis; Hoechst 33342; cell apoptosis; western blotting



Preprints.org is a free multidisciplinary platform providing preprint service that is dedicated to making early versions of research outputs permanently available and citable. Preprints posted at Preprints.org appear in Web of Science, Crossref, Google Scholar, Scilit, Europe PMC.

Copyright: This open access article is published under a [Creative Commons CC BY 4.0 license](#), which permit the free download, distribution, and reuse, provided that the author and preprint are cited in any reuse.

Disclaimer/Publisher's Note: The statements, opinions, and data contained in all publications are solely those of the individual author(s) and contributor(s) and not of MDPI and/or the editor(s). MDPI and/or the editor(s) disclaim responsibility for any injury to people or property resulting from any ideas, methods, instructions, or products referred to in the content.

Article

# From Functional Food to Therapeutic Prospect: Mechanistic Study of Gypenoside XVII in HeLa Cells

Sayed Sajid Hussain <sup>1</sup>, Muhammad Maisam <sup>1</sup>, Shoaib Younas <sup>2</sup>, Feng Wang <sup>1,\*</sup> and Weijie Li <sup>2,\*</sup>

<sup>1</sup> School of Food Science and Biological Engineering, Hefei University of Technology, Hefei 230009, P.R. China

<sup>2</sup> School of Health Science and Engineering, University of Shanghai for Science and Technology, Shanghai 200093, P.R. China

\* Correspondence: fengw420@hfut.edu.cn (F.W.); 13651731551@139.com (W.L.)

## Abstract

Cervical cancer remains a prominent cause of cancer-related mortality among women worldwide because of chronic infection with high-risk human papillomavirus (HPV) and disparate access to prevention and treatment. The current research evaluates the anticancer activity of Gypenoside XVII, a bioactive saponin of *Gynostemma pentaphyllum*, in HeLa cells as a model of cervical cancer. MTT, Annexin V-PI, and Hoechst 33342 assays showed dose-dependent growth inhibition with typical apoptotic morphology. Flow cytometry revealed G<sub>0</sub>/G<sub>1</sub> cell-cycle arrest, while pathway interrogation revealed participation of mitochondrial and death-receptor cascades, in agreement with caspase-9 and caspase-8 activation, respectively. Collectively, these findings position Gypenoside XVII as a natural-product bioactive with potential both as an anticancer lead and as a functional-food ingredient, deserving of further preclinical development.

**Keywords:** Gypenoside XVII; HeLa; cell cycle analysis; Hoechst 33342; cell apoptosis; western blotting

## 1. Introduction

Cancer remains one of the world's leading health crises and kills more individuals than stroke and other cardiovascular disorders, says the World Health Organization (<https://www.who.int/cancer/prevention/en/>). Its incidence continues to increase everywhere across the globe due to aging and moving populations, with a projection of as many as 35 million cases by 2050, especially in the less developed world. The 2022 global report estimates nearly 20 million incident cases and 9.7 million deaths [1], a rising burden with differences across regions and health systems. Differences in the distribution of cancer types and delayed presentations are the explanations for high mortality rates in Asia and Africa, where case fatality rates are high. Though Europe has only 9.6% of the global population, it accounts for 22.4% of new cancer cases and 20.4% of cancer mortality, which indicates a high regional burden based on the prevalence of cancer types and economic limitations in healthcare [2]. Of particular notable concern is cervical cancer, the third most common cancer and killer of women [3], for which 13,960 new cases and 4,310 deaths are estimated globally in 2023. Estimates also predict 528,000 new cases by 2026, 85% of which will occur in developing countries [4].

Different modalities of therapy have been employed for cancer treatment; yet, scientists continue to search for more accessible and effective procedures. Anticancer potential of medicinal plants has been reported to be of considerable interest. Among them, *Gynostemma Pentaphyllum* Makino, or "Jiao Gu Lan" in Chinese, is a species of genus *Gynostemma* Bl belonging to the family of Cucurbitaceae and extensively distributed plant of Northeast and Southeast Asia is best recognized for its disease resistance [5–8]. Other than its pharmacological potential, *G. Pentaphyllum* has been used for a very long time in China as an ingredient of food items and health foods, such as beverages, noodles, cookies, bath supplies, and cosmetics. Its original habitat is primarily found in the southern parts of

the both Yangtze River and Qinling Mountains [9,10]. It has been applied to treat numerous disorders in the past, such as hematuria, pharynx pain, edema, neck inflammation, and trauma [11]. In recent times, *G. pentaphyllum* has also attracted international attention, and products ranging from powders, teas, tablets, capsules, oral solutions, and pills to reach the benefits are available on the open market within the United States, China, and other Asian and European nations [12–14]. Furthermore, recent research has demonstrated its broad pharmacological promise from anticancer, antibacterial, anti-aging, anti-fatigue, and anti-ulcer to hypolipidemic and immunomodulatory activities [15–18]. It contains a variety of bioactive compounds such as saponins [19], carotenoids [20], flavonoids [9], chlorophylls [21], lignins [22], and polysaccharides [23]. Amongst them, saponins, also referred to as gyno-saponins or gypenosides, are of particular interest with over 280 types. These saponins are regarded as the functional basic elements responsible for most of the plant's diverse biological functions [24].

Gypenosides anticancer activity has been investigated on diverse cancer cell lines, including Eca-109 (esophageal), SW620 (colon), SAS (oral), and cervical epidermoid carcinoma [25–27]. Further research needs to be performed to comprehensively demonstrate the antitumor action of gypenosides of *G. pentaphyllum*. The present paper reports the strong action of Gypenoside XVII in anticancer therapy, inspired by the activity of *G. pentaphyllum* saponins. This research represents the first report of anticancer effects of Gypenoside XVII and delivers a novel therapeutic strategy, with experimental evidence in human cervical carcinoma cells (HeLa cells) for future studies and clinical trials.

## 2. Results

**Inhibition Effect of Gypenoside XVII on HeLa Cell Proliferation.** The MTT assay, performed to evaluate the in vitro cytotoxic effects of drugs and other research elements on cell lines or primary patient cells, is extensively employed in cancer research to detect mitochondrial function in live cells. The process relies on the reduction of 3-[4,5-Dimethylthiazol-2-yl]-2,5-diphenyl tetrazolium bromide (MTT) to crystalline formazan [28]. The effect of Gypenoside XVII on HeLa cells has been evaluated using the MTT assay, and the findings indicated a dose-dependent inhibitory effect. Following a 24-hour exposure to Gypenoside XVII, the reduction in cell proliferation was found to escalate with higher drug concentrations. The  $IC_{50}$  value, denoting the concentration necessary to inhibit 50% of cell proliferation, was determined to be 133.39  $\mu$ M through curve fitting as shown in Figure 1a. As a positive control, 5-FU exhibited an inhibition rate of 55.24%. Figure 1b comprehensively shows the inhibitory effects of Gypenoside XVII on HeLa cells.

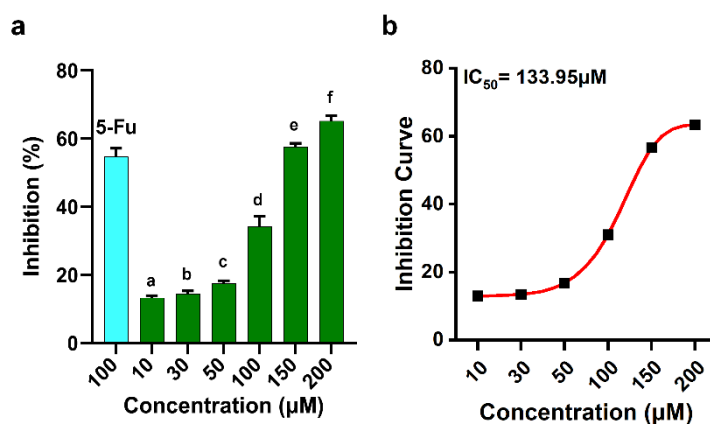


**Figure 1.** HeLa cell growth is inhibited by 5-FU and Gypenoside XVII. (a) The dose-response inhibition curve of Gypenoside XVII on HeLa cells, featuring the  $IC_{50}$  value, indicates the concentration at which Gypenoside XVII attains 50% inhibition. (b) Rate of inhibition, and a concentration of 100  $\mu$ M 5-FU served as a positive internal control. All treated cells underwent incubation for 24 hours. Data are expressed as the mean  $\pm$  SD from three different experiments and analyzed via one-way ANOVA, with significance established at  $p < 0.05$ .

**Effect of Gypenoside XVII on Cell Cycle.** Cell cycle is the prominent phenomena in apoptotic study and consists of different phases such as  $G_0/G_1$  phase, S phase, G2 phase, and M phase. In current study flow cytometry was utilized to assess the inhibitory effect of Gypenoside XVII on HeLa cells. Figure 2a shows that Gypenoside XVII administration resulted in a significant increase in cell accumulation in the  $G_0/G_1$  phase compared to the control group, although the percentage of cells in the S and G2/M phases decreased. Figure 2b shows the dispersion of cells over different phases. Following a 24-hour treatment of HeLa cells with varying concentrations of Gypenoside XVII, there was a progressive increase in the suppression of cell numbers in the  $G_0/G_1$  phase (untreated 57.70%, 90  $\mu$ M 61.59%, 130  $\mu$ M 70.01%, and 150  $\mu$ M 75.12%), while a decline was observed in the S and G2/M phases.

The Figure 2c–e depict the molecular regulation of gypenoside XVII on cell cycle-related genes and protein through western blotting and real-time PCR to elucidate the underlying mechanisms. The cyclin E/CDK2 complex significantly governs cellular control during the  $G_0/G_1$  phase [29]. Cells treated with gypenoside XVII exhibited a dose-dependent elevation in mRNA expression. Notably, mRNA levels of Cyclin B, Cyclin E, CDK2, CDK6, p16, and p21 were all augmented. Furthermore, gypenoside XVII similarly affected protein expression levels, thereby providing substantial evidence for its regulatory role on the cell cycle in HeLa cells. These results show that Gypenoside XVII impeded the progression and synchronization of cell cycle stages, resulting in cell cycle arrest at the  $G_0/G_1$  phase.

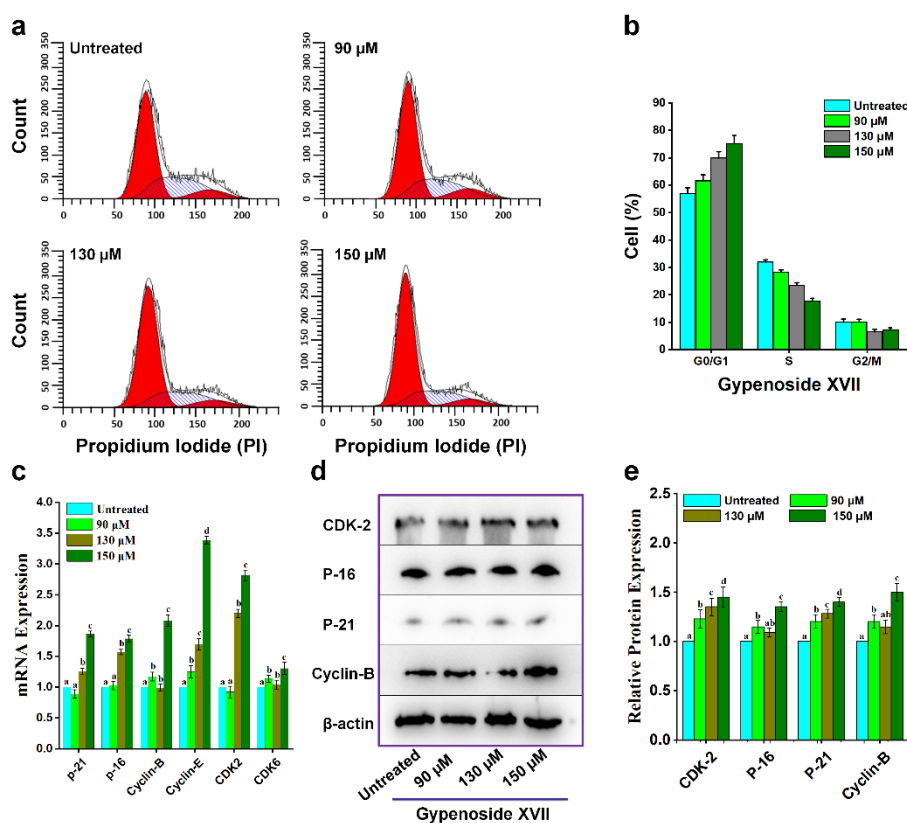


**Figure 2.** Cell cycle distribution was examined using flow cytometry. (a) Distribution of HeLa cells among the  $G_0/G_1$ , S, and G2/M phases following treatment with different doses of Gypenoside XVII. (b) Percentage of cells in each phase of the cell cycle across various treatment conditions. One-way ANOVA was utilised for statistical analysis. Fig 2c, 2d, and 2e exhibit HeLa cells treated with and without Gypenoside XVII were subjected to RT-PCR and Western blotting to assess the expression levels of cell cycle-related genes and proteins. (c) RT-PCR data indicating the expression levels of cell cycle-associated genes in HeLa cells subjected to treatment with and without Gypenoside XVII. Western blot analysis (d, e) demonstrating the impact of Gypenoside XVII on cell

cycle-associated proteins in HeLa cells. All data are expressed as mean  $\pm$  SD from three independent experiments, with statistical significance assessed via one-way ANOVA ( $p < 0.05$ ).

**Effect of Gypenoside XVII on HeLa Cell Apoptosis.** Based on our previous investigations demonstrating that the Stevenleaf of *G. pentaphyllum* induced apoptosis in human hepatoma HepG2 cells [30], We found that Gypenoside XVII also caused cervical cancer HeLa cells to undergo apoptosis. In our analysis, HeLa cells were treated with Gypenoside XVII at different concentrations (0  $\mu$ M, 90  $\mu$ M, 130  $\mu$ M, and 150  $\mu$ M). Following a 24-hour incubation period, the treated cells were stained with Annexin V-FITC solution, and apoptotic activity was measured by flow cytometry. The findings demonstrated that, especially in the lower-right quadrant of the FCM plots, which indicates early apoptosis, the treated groups' apoptotic cell ratio considerably increased as compared to the untreated cells. The results demonstrated that Gypenoside XVII induces early apoptosis in HeLa cells, as seen in Figure 3a–d.

In the same vein, this phenomenon was further verified by utilizing Hoechst 33342, a bis-benzimide derivative from the Hoechst family, comprises Hoechst Red (630-650 nm) and Hoechst Blue (405-450 nm). Additionally, these dyes selectively bind to AT-rich regions of double-stranded DNA within the minor groove and is extensively utilized for assessing nuclear integrity, apoptotic rates, and cell cycle phases at the microscopic level. Fluorescence intensity in cell populations varies with dye absorption, which increases with concentration; as absorption rises, fluorescence transitions from blue to red, indicating the ratio of necrotic to apoptotic cells [31,32]. Apoptosis was validated by our analysis, revealing a notable increase in blue fluorescence in apoptotic cells compared to untreated cells. Necrosis, characterised by compromised membrane integrity, is indicated by DNA leakage from ruptured cell membranes, as evidenced by red fluorescence, a marker of PI staining. As illustrated in Figure 3e–h, the intensity of red fluorescence markedly increased with elevated doses of Gypenoside XVII.

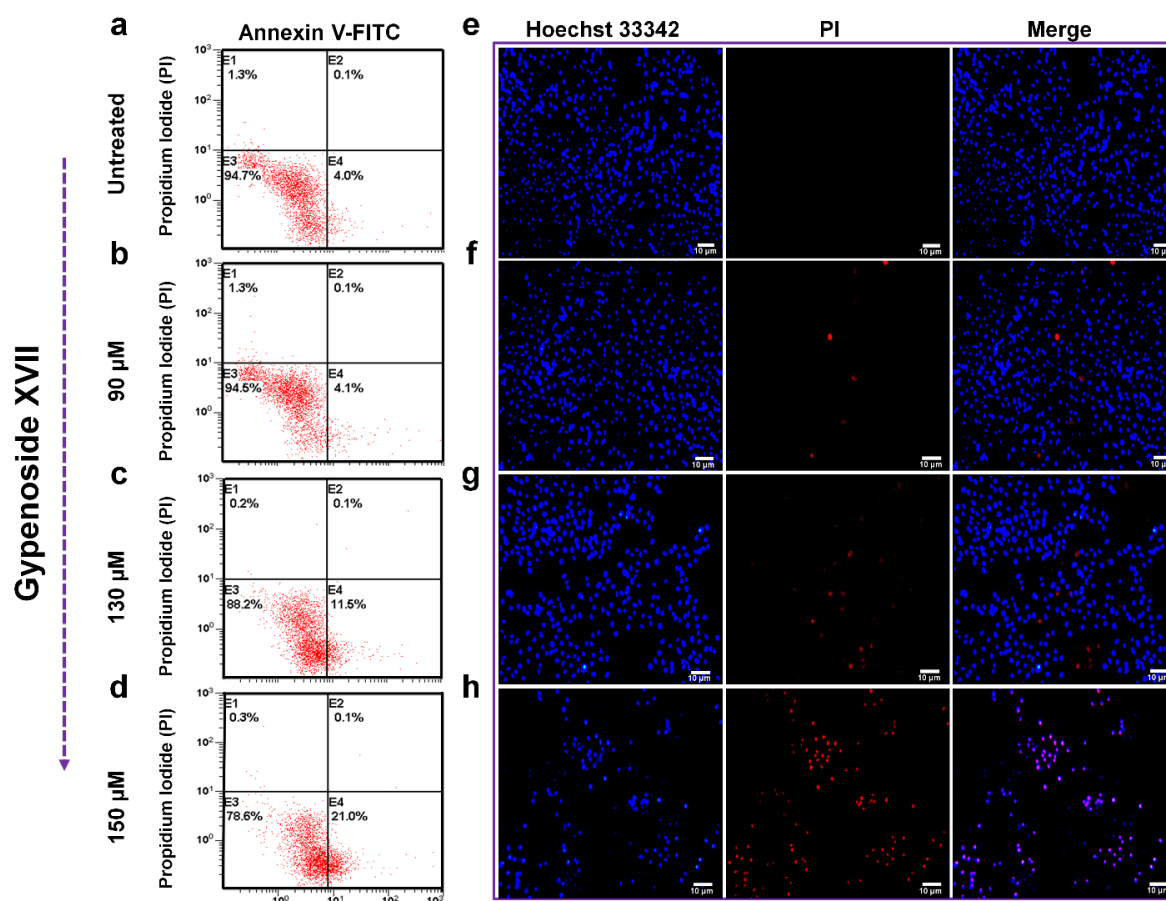


**Figure 3.** Annexin V-PI labelling followed by flow cytometry (FCM) analysis to assess apoptosis and Hoechst 33342 staining was used to detect apoptotic cell death morphology in HeLa cells treated with Gypenoside XVII for 24 hours. Results are shown for the subsequent treatment groups: (a): Untreated; (b): 90  $\mu$ M; (c): 130  $\mu$ M; (d): 150  $\mu$ M for Annexin V-PI labelling, and (e): Untreated; (f): 90  $\mu$ M; (g): 130  $\mu$ M; (h): 150  $\mu$ M. Scale bar: 10 $\mu$ M for Hoechst 33342 staining.

**Effect of Gypenoside XVII on Mitochondrial Pathway-Related Genes.** Apoptosis is essential in normal ageing, development, cancer progression, and neurological disorders such as amyotrophic lateral sclerosis, Alzheimer's disease, and Parkinson's disease [33]. The two principal routes that trigger apoptosis are the Mitochondrial Pathway (intrinsic pathway) and the Death Receptor Pathway (extrinsic pathway). Both pathways culminate in the activation of caspases, the ultimate executors of cell death [34]. The Mitochondrial Pathway is especially crucial in reaction to cellular factors including ischaemia, DNA damage, and oxidative stress. The process entails the permeabilization of the mitochondrial outer membrane through the permeability transition pore, ultimately resulting in cell death. Our analysis revealed that Gypenoside XVII administration resulted in the increase of mRNA expression levels for Caspase-3, Caspase-9, Cytochrome-c, Bax, Puma, and Smad, whereas the expression levels of Bad and BCL-2 were downregulated (Figure 4a). The findings were corroborated by Western blot analysis, which validated the alterations in protein expression levels (Figure 4b–e).

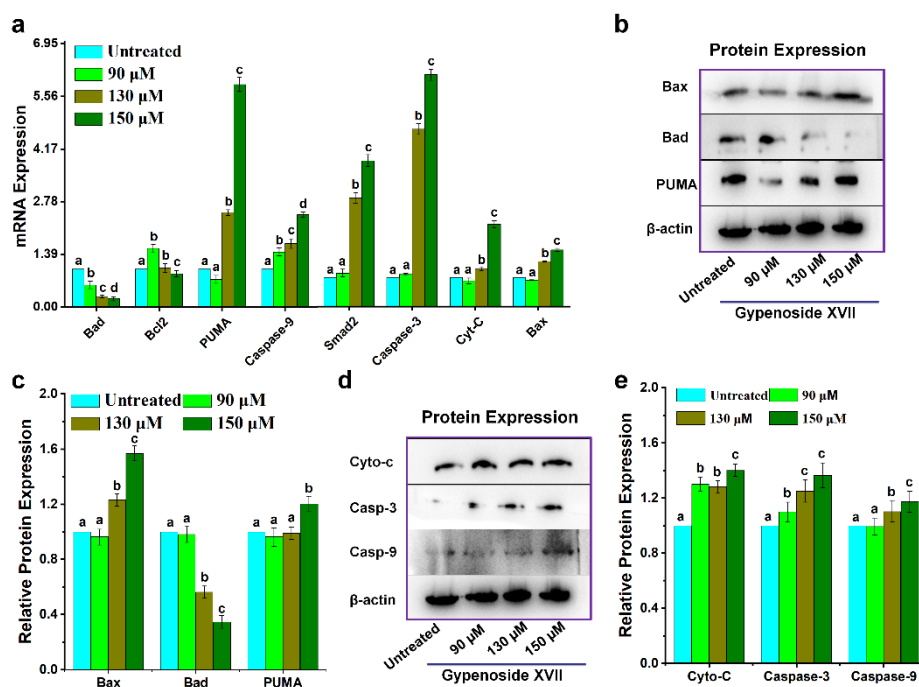


**Figure 4.** The expression levels of genes and proteins linked to the mitochondrial pathway were examined in HeLa cells treated with Gypenoside XVII at concentrations of 90  $\mu$ M, 130  $\mu$ M, 150  $\mu$ M, and 0  $\mu$ M (untreated). (a) Expression levels of mRNA for genes associated with the mitochondrial pathway following 24 hours of Gypenoside XVII administration. (b, c, d, e) Protein expression levels of mitochondrial pathway-associated proteins in HeLa cells treated with Gypenoside XVII. All data are expressed as mean  $\pm$  standard deviation from three independent experiments. Statistical analysis was conducted utilising one-way ANOVA ( $p < 0.05$ ).

**Effect of Gypenoside XVII on Death Receptor Pathway.** As members of the tumour necrosis factor (TNF) superfamily, these cell surface receptors can bind ligands and induce apoptosis. These receptors employ both internal and extrinsic processes to trigger apoptosis. Gypenoside XVII administration of the extrinsic pathway markedly elevated the mRNA and protein expression levels of FADD, Caspase-8, Caspase-10, and DR5 in our investigation, while TNF-R1 expression

dramatically diminished after 24 hours, as illustrated in Figure 5a. The Western blot analysis, illustrated in Figure 5b,c, corroborated these observations about protein expression.

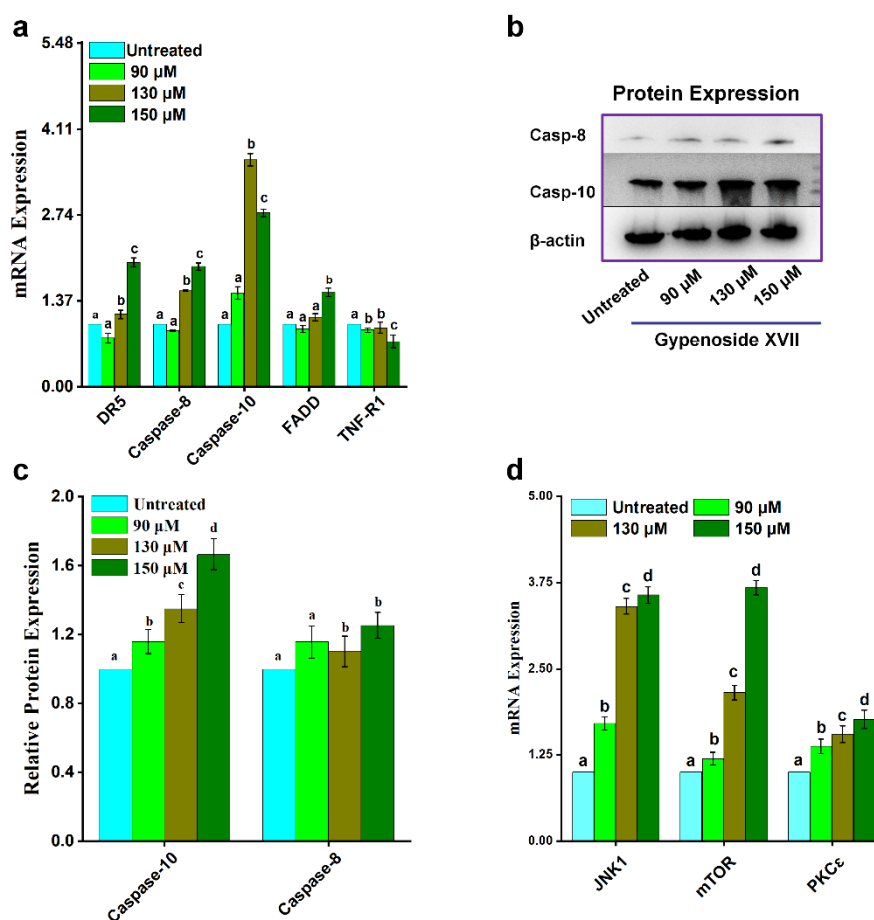


**Figure 5.** Gypenoside XVII's effects on HeLa cells include changes in the death receptor pathway and other genes linked to apoptosis. (a) mRNA expression levels of genes associated with the death receptor pathway. (b) Protein expression levels of the identical pathway. (c) Gene expression levels of additional apoptosis-related pathways in HeLa cells subjected to varying doses of Gypenoside XVII.

**Effect of Gypenoside XVII on Other Apoptosis-Related Genes.** Besides its impact on the Death Receptor Pathway, Gypenoside XVII also affected the mRNA expression of genes associated with other apoptosis pathways. Treatment of HeLa cells with Gypenoside XVII led to a notable overexpression of JNK1, mTOR, and PKC $\epsilon$ , indicating that supplementary pathways are involved in the apoptotic process. The results are illustrated in Figure 5d.

### 3. Discussion

Combating against cancer continues to be a persistent issue, requiring the use of advanced techniques to effectively combat this potentially fatal disease. The development of novel pharmaceuticals with enhanced selectivity and reduced toxicity has emerged as a global objective in cancer prevention and therapeutic personalization. In this context, Gypenoside XVII derived from *G. pentaphyllum* has increased attention due to its putative anticancer properties, and hence in this study the molecular mechanisms of Gypenoside XVII in HeLa cells were examined. The flow cytometry study revealed that Gypenoside XVII administration significantly increased the accumulation of HeLa cells in the G<sub>0</sub>/G<sub>1</sub> phase of the cell cycle, underscoring its impact on this essential checkpoint. Thus, Cyclin-D activates CDK4 and CDK6, governing cell development during the G1 phase,

whereas Cyclin-A and Cyclin-E activate CDK2 to regulate chromosome replication during the cell cycle [35]. Karimian et al. claim that the p21 gene, part of the CDK inhibitor family, is essential for the regulation of the cell cycle, DNA replication, repair, and tumor suppression. The p21, CDK1, and Cyclin-B1 complex collectively impede CDK activation, resulting in cell cycle arrest [36]. The p16 tumor suppressor gene specifically binds to CDK4 and CDK6, inhibiting their interaction with Cyclin-D. The inhibitor obstructs the phosphorylation of retinoblastoma (Rb) protein, thereby producing cell cycle arrest in the G<sub>1</sub> phase upon overexpression of p16 [37,38]. Our findings demonstrated the same phenomena and based on our findings and referenced data, we infer that Gypenoside XVII induces cell cycle arrest at the G<sub>0</sub>/G<sub>1</sub> phase via the p16, p21, and Cyclin-E pathways [39]. Apoptosis, a critical process in cancer research, regulates cellular development and reactions to environmental stimuli. Flow cytometry data indicated that Gypenoside XVII administration prompted apoptosis, especially in the early apoptotic phase. After 24 hours of exposure to Gypenoside XVII, the ratio of cells in the early apoptotic phase rose from 4.1% to 21.0%.

Similarly, for further justification the effect of Gypenoside DVII on Death Receptor Pathway and the Mitochondrial Pathway were examined. Our investigation revealed that Gypenoside XVII markedly enhanced the mRNA expression of TNF-R1, FADD, Caspase-8, Caspase-10, and DR5. The TNF superfamily cytokines initiate signaling pathways essential for cell survival, differentiation, and death. TNF-R1 triggers apoptosis and is internalized following TNF binding, resulting in the dissociation of the TRADD complex and the recruitment of FADD. This mechanism stimulates Pro-Caspase-8 and generates the death-inducing signaling complex (DISC), so beginning apoptosis through the extrinsic pathway [40,41].

The BCL2 family, which consists of pro-apoptotic, anti-apoptotic, and BH3-only proteins, is responsible for the control of the mitochondrial pathway of apoptosis [42,43]. The BCL2 family member Puma, which promotes apoptosis, is essential to this process. Liu et al. reported that an in vitro study indicated Puma overexpression correlates with elevated BAX expression, structural alterations in BAX, and its relocation to the mitochondrial membrane. Cytochrome-c is released as a result of these processes, which lower the potential of the mitochondrial membrane [43]. Our results indicated substantial alterations in the expression of Bax and BCL-2, accompanied by elevated Puma expression (a BH3-only protein). This chain of events increased mitochondrial membrane permeability, facilitating cytochrome c release to the cytosol. Consequently, cytochrome-c upregulated Caspase-9 expression, which subsequently activated Caspase-3, ultimately initiating apoptosis. To elucidate these findings, a flowchart was constructed Figure 6, illustrating the anticipated anticancer mechanism of Gypenoside XVII, that includes cell cycle arrest and apoptosis induction.

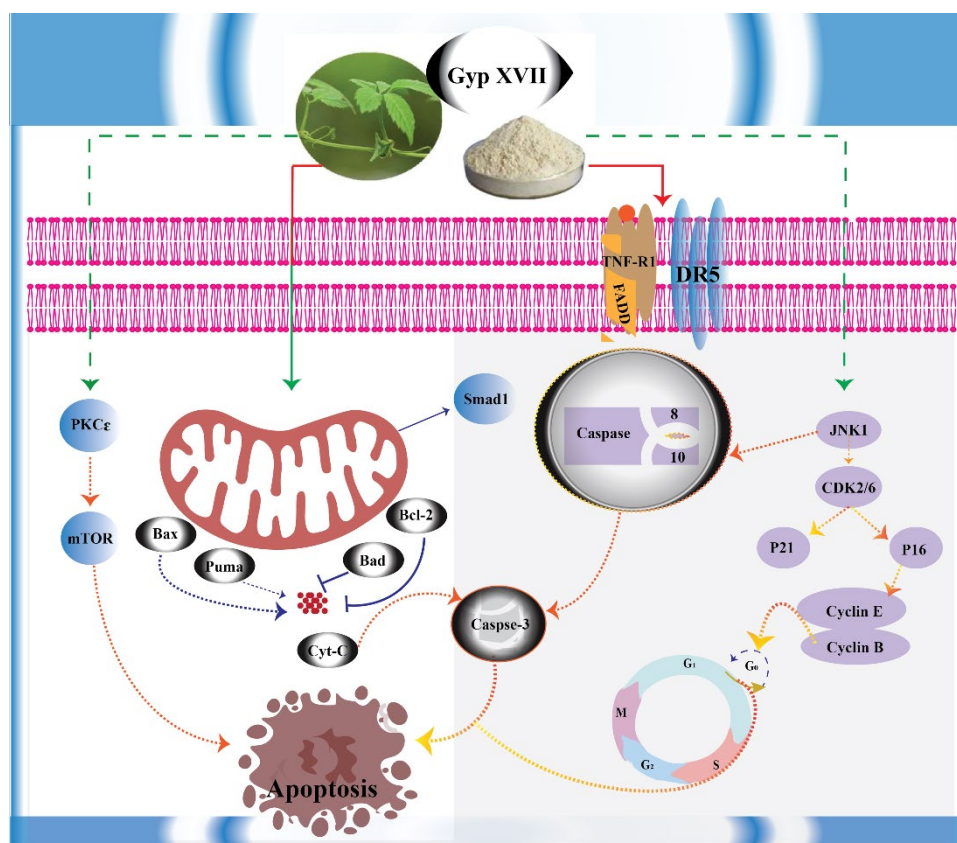


**Figure 7.** Proposed molecular mechanism of Gypenoside XVII treatment in HeLa cells.

#### 4. Experimental Method

**Chemicals and reagents.** Gypenoside XVII was obtained from Chengdu Must Bio-Technology Co., Ltd., PR China (molecular weight: 947.15 g/mol; purity: 99.6%). All chemical reagents, including ribonuclease-A, Tris HCl, potassium phosphate, and propidium iodide (PI), were sourced from Shanghai Sinopharm Chemical Reagent Co., Ltd., Shanghai, China. Pencillin-streptomycin, glutamine, fetal-bovine serum (FBS), Dulbecco's Modified-Eagle's Medium (DMEM), and trypsin-EDTA were purchased from Invitrogen (Carlsbad, CA, USA). Specific inhibitors of caspase-3 and caspase-8 were acquired from Med Chem Express, located in Monmouth Junction, New Jersey, USA.

**Cell Preparation.** A human cervical cancer cell-line called HeLa cells were purchased from Shanghai Wei Atlas Biological Technology Co., Ltd. (Shanghai, China). All experiments were carried out under observation. The DMEM media supplemented with 6 mM glutamine, 100 U/mL penicillin, 100 µg/mL streptomycin, and 10% FBS was used to culture the cells. To promote the best possible adhesion to the plates, the cells were incubated for 24 hours at 37°C in an atmosphere with 5% CO<sub>2</sub> and 95% air.

**MTT Assay.** After HeLa cells were seeded and incubated for 12 hours, 100 µL of the cell suspension ( $5 \times 10^4$  cells/well) was added to each well of a 96-well plate. 50 µM 5-fluorouracil (5-FU) served as a positive control before gypenoside XVII was given at various dosages (0 µM, 10 µM, 30 µM, 50 µM, 100 µM, 150 µM, and 200 µM). For a whole day, the plates were incubated. Following the addition of 20 µL of 5 mg/mL MTT reagent to each well, the plates were incubated for an additional 4 hours. The generated formazan-crystals were then dissolved by using 150 µL of DMSO. At 570 nm, the absorbance was measured with the help of microplate reader [28].

**Cell Cycle Analysis.** Following that, six-well plates were seeded with  $3 \times 10^5$  Hela cells. After 12 hours, several quantities of Gypenoside XVII were added: 0 µM, 70 µM, 90 µM, 110 µM, 130 µM, and 150 µM. Trypsinization was used to harvest the treated and normal cells following a 24-hour incubation period at 37°C in a CO<sub>2</sub> incubator. After being rinsed with 1× phosphate-buffered saline

(PBS), the cells were gradually fixed by adding 70% ethanol and kept at 4°C for the entire night. After that, the cells were reconstituted in PI solution and allowed to sit in the dark for thirty minutes. In the end, the samples were examined using flow cytometry (BD Accuri C6, USA) with a 488 nm excitation wavelength [44].

**Cell Apoptosis.** Cell-apoptosis was assessed by Annexin V-FITC double staining (Beyotime, Shanghai, China) in agreement with the manufacturer's instructions. Following the experiment, treated cells at a concentration of  $1 \times 10^6$  cells/mL were resuspended in 1x Annexin binding solution. After treating the cells with 5  $\mu$ L of Annexin V-FITC and 10  $\mu$ L of PI, they were incubated at 2-8°C for 15 and 5 minutes, respectively. Flow cytometry (FCM) was then used to identify apoptotic cells [45].

**Measurement of Apoptotic Morphology.** We used Hoechst 33342-PI staining to analyze the apoptotic morphology of HeLa cells. Gypenoside XVII was administered to HeLa cells ( $1 \times 10^6$  cells/mL) at concentrations of 0  $\mu$ M, 90  $\mu$ M, 130  $\mu$ M, and 150  $\mu$ M. The cells were incubated for 24 hours, then washed with 1x PBS and stained with Hoechst 33342 and 5  $\mu$ L of PI staining solution. Before analysis, the samples were washed twice with 1x PBS after being incubated for 20 minutes. Finally, laser-confocal microscopy (Carl-Zeiss Microscopy GmbH, Jena, Germany) was used to detect red and blue fluorescence.

**RT-qPCR Analysis.** As highlighted in our previous studies [46], HeLa cells were subjected to treatment with different concentrations of Gypenoside XVII (0  $\mu$ M, 90  $\mu$ M, 130  $\mu$ M, and 150  $\mu$ M) to measure the expression of genes associated with the cell cycle and apoptosis. Whole RNA was extracted with RNAiso Plus reagent (TaKaRa, Dalian Company, Ltd., Liaoning, China) in accordance with the manufacturer's guidelines. The RNA was further processed to eliminate DNA and reverse-transcribed into cDNA utilizing the Takara Reverse kit. Quantitative PCR (qPCR) was conducted utilizing the LightCycler 96 System (Roche, Basel, Switzerland), with  $\beta$ -actin as the internal control. The nucleotide sequences employed in this study are specified in Table 1.

**Table 1.** Primers for RT-PCR.

Genes	Primers	Sequences	Genes	Primers	Sequences
Caspase-3	Forward	TGGACTGTGGCATTGAGAA	FADD	Forward	GGGAAGAAGACCTGTGTGCA
	Reverse	CAGGTGCTGTGGAGTATGCA		Reverse	ATTCTCAGTGACTCCCGCAC
p-21	Forward	GCGGAACAAGGAGTCA GACA	Cyclin-E	Forward	GGATTATTGCACCATCCAGAGGCT
	Reverse	GAACCAGGACACATGGGGAG		Reverse	CTTGTGTCGCCATATAACCGGTCAA
p-16	Forward	CTTCCTGGACACGCTGGT	Cyclin-B1	Forward	CTGCTGGGTGTAGGTCCTTG
	Reverse	ATCTATGCGGGCATGGTTACT		Reverse	TGCCATGTTGATCTTCGCTT
Cyt-c	Forward	AGGAGGTGGAGGCAAA GGTA	PKC $\epsilon$	Forward	TGCCCCACAAGTTCGGTATC
	Reverse	ATATTTGCACAGTGAAACATAGGA		Reverse	GCCGCTGTTGGTGATTTTGT
TNF-R1	Forward	CTCTCCCCTCCTCTCTGCTT	mTOR	Forward	TTATGGGCAGCAACGGACAT
	Reverse	GGTTGAGACTCGGGCATAG		Reverse	CTTCTCCCTGTAGTCCCGGA
Caspase-10	Forward	CAGGGGCAGGAAGAGACACAG	JNK1	Forward	ACATTGAGCAGAGCAGGCAT
	Reverse	ACTAGGAAACGCTGCTCAC		Reverse	GTCAGGAGCAGCACCATTCT

<b>Caspase-8</b>	Forward	TATCCCGGATGGCTGAC T	<b>Bcl-2</b>	Forward	GGAGCGTCAACAGGGAGA TG
	Reverse	GACATCGCTCTCAGGCT C		Reverse	GATGCCGGTTCAGGTACTC AG
<b>Smad1</b>	Forward	GGCCTCACGTCATCTAC TGCC	<b>Puma</b>	Forward	ATGCCTGCCTCACCTTCAT C
	Reverse	GGGTTACGGAA- GCGTGGCAGCAT		Reverse	TCAGCCAAAATCTCCCACC C
<b>CDK-6</b>	Forward	CGGGATCCACCATGGA GAAGGACGGCCTG	<b>Bax</b>	Forward	AGTAACATGGAGCTGCAG AGG
	Reverse	CGGATCCATTGCTCAGG CTGTATTCAGCTCCGA		Reverse	ATGGTTCTGATCAGTTCCG G
<b>CDK2</b>	Forward	CTTTGGAGTCCCTGTCC GTA	<b>Bad</b>	Forward	AGAGTTTGAGCCGAGTGA GC
	Reverse	CGAAAGATCCGGAAGA GTTG		Reverse	CATCCCTTCGTCGTCCTCC
<b>DR5</b>	Forward	CGTCCGCATAAATCAGC ACG	<b><math>\beta</math>-actin</b>	Forward	TGTGATGGTGGGAATGGGT CAG
	Reverse	TCTGTCCCCGTTGTTCCA TG		Reverse	TTTGATGTCACGCACGATT TCC

**Western Blotting Analysis.** HeLa cells were cultivated for 24 hours after being seeded at a density of  $1 \times 10^6$  cells per well. For a full day, cells were exposed to several doses of Gypenoside XVII (0  $\mu$ M, 90  $\mu$ M, 130  $\mu$ M, and 150  $\mu$ M). Following the manufacturer's instructions, proteins were isolated using a protein extraction kit. The samples were mixed with 2x loading buffer after protein measurement, and they were then heated for 10 minutes. Using 10% SDS-PAGE electrophoresis (Rebio, Shanghai, China), the target proteins were separated and then moved to a polyvinylidene difluoride (PVDF) membrane (Millipore, Darmstadt, Germany). Using primary antibodies (Cell Signaling Technology), the membrane was treated with 5% skim milk for two hours at room temperature and then overnight at 4°C. Secondary antibodies were subsequently given. The internal reference was  $\beta$ -actin. ECL luminescence was used to identify protein bands, and grayscale imaging was then used for analysis (Transgen, Beijing, China) [29].

**Statistical Analysis.** SPSS software (SPSS, Inc., Chicago, IL, USA) was used for data analysis. One-way analysis of variance (ANOVA) was employed to identify differences between Gypenoside XVII treatment groups, with statistical significance set at  $p < 0.05$ .

## 5. Conclusions

In summary, this research shed light about the *in vitro* anticancer activity of Gypenoside XVII as a bioactive saponin, against HeLa cells, characterized by impaired cell proliferation, G0/G1 arrest, and coordinated activation of intrinsic and extrinsic apoptosis, thereby placing it from a functional food constituent to a therapeutic lead scaffold. Given these results, Gypenoside XVII emerges as a promising anticancer agent worthy of detailed pharmacodynamic, pharmacokinetic, and safety testing in appropriate *in vivo* models with subsequent verification against a broad range of cervical cancer subtypes and comparator standards-of-care to establish translational feasibility. Future studies should distinguish between target engagement and pathway hierarchy (e.g., BCL2 family regulation, caspase cascades, and death receptor signaling), probe combinatorial regimens to enhance efficacy or overcome resistance, and assess formulation strategies that increase bioavailability and tumor delivery. Collectively, these steps will establish therapeutic index and clinical positioning, advancing Gypenoside XVII from mechanistic proof-of-concept toward preclinical development as an effective anticancer agent against cervical cancer.

**Author Contributions. Study conception and design:** Feng Wang designed the study and revised the manuscript, data collection: Sayed Sajid Hussain collected the whole data, analysis and interpretation of results: Sayed Sajid Hussain, Shoaib Younas analyzed the results, draft manuscript: Zhao-Jun Wei, and Weijie Li approved the final submission of the manuscript. The final version was also verified and approved by all authors.

**Funding:** This research was supported by the National Natural Science Foundation of China (82170481), and the Key Research and Development Plan of Anhui Province (202104b11020015).

**Availability of data and materials:** All the data and information related to this study are described elaborately in the paper.

**Acknowledgments:** We would like to thank the authors who participated in the research project.

**Conflict of interest:** There is none to declare.

## References

1. American Cancer Society. (2022). Global cancer facts & figures 4th edition. In: ; 2022. <https://www.cancer.org/research/cancer-facts-statistics/global-cancer-facts-and-figures.html>
2. Bray, F.; Laversanne, M.; Sung, H.; Ferlay, J.; Siegel, R.L.; Soerjomataram, I.; Jemal, A. Global cancer statistics 2022: GLOBOCAN estimates of incidence and mortality worldwide for 36 cancers in 185 countries. *CA Cancer J Clin.* 2024;74 (3):229-263.
3. Ma, Y.L.; Zhang, Y.S.; Zhang, F.; Zhang, Y.Y.; Thakur, K.; Zhang, J.G.; Wei, Z.J. Methyl protodioscin from *Polygonatum sibiricum* inhibits cervical cancer through cell cycle arrest and apoptosis induction. *Food and Chemical Toxicology.* 2019; 132:110655.
4. Sekar, P.K.C.; Thomas, S.M.; Veerabathiran, R. The future of cervical cancer prevention: advances in research and technology. *Explor Med.* 2024; 5(3):384-400.
5. Ahmad, B.; Khan, S.; Nabi, G.; Gamallat, Y.; Su, P.; Jamal, Y.; Duan, P.; Yao, L. Natural gypenosides: targeting cancer through different molecular pathways. *Cancer Manag Res.* 2019;11:2287-2297.
6. Bokelmann, J.M. *Gynostemma/Jiaogulan (Gynostemma Pentaphyllum)*. Elsevier eBooks; 2022.
7. Quang, H.T.; Thi, P.; Sang, D.N.; Tram, T.T.N.; Huy, N.D.; Dung, T.Q.; The, Q.T.T. Effects of Plant Elicitors on Growth and Gypenosides Biosynthesis in Cell Culture of *Gynostemma pentaphyllum*. *Molecules.* 2022; 27(9):2972.
8. Wang, J.; Yang, J.L.; Zhou, P.P.; Meng, X.H.; Shi, Y.P. Further new gypenosides from *Jiaogulan (Gynostemma pentaphyllum)*. *J Agric Food Chem.* 2017; 65(29):5926-5934.
9. Zhen-xing, WANG.; Jin-mei, YANG.; Zhi-bin, ZHANG.; Xiao-tian ZHU.; Ping XIANG.; Jian, SUN.; Xia-hong, HE. Chemical constituents and biological activity of *Gynostemma pentaphyllum*: A review. *Journal of Southern Agriculture.* 2023;54(6):1741-1752.
10. Ji, X.; Shen, Y.; Guo, X. Isolation, structures, and bioactivities of the polysaccharides from *Gynostemma pentaphyllum* (Thunb.) Makino: A review. *BioMed research international.* 2018; (1):6285134.
11. Su, C.; Li, N.; Ren, R.; Wang, Y.; Su, X.; Lu, F.; Ma, X. Progress in the medicinal value, bioactive compounds, and pharmacological activities of *Gynostemma pentaphyllum*. *Molecules.* 2021; 26(20):6249.
12. Ahmed, A.; Saleem, M.A.; Saeed, F.; Afzaal, M.; Imran, A.; Nadeem, M.; Ambreen, S.; Imran, M.; Hussain, M.; Al Jbawi, E. *Gynostemma pentaphyllum* an immortal herb with promising therapeutic potential: a comprehensive review on its phytochemistry and pharmacological perspective. *Int J Food Prop.* 2023;26(1):808-832.
13. Anuradha, B.; Vaibhav, C. *Gynostemma pentaphyllum* extract market: Trends & growth analysis. 2024; 2032.
14. Yuge, N.; Wei, Y.; Junli, L.; Wenbing, Y.; Liangli, Y. Characterization of a Novel Polysaccharide from Tetraploid *Gynostemma pentaphyllum* Makino. *J Agric Food Chem* 2013; 61(20):4882-4889.
15. Deng, Q.; Yang, X. Protective effects of *Gynostemma pentaphyllum* polysaccharides on PC12 cells impaired by MPP(+). *Int J Biol Macromol.* 2014; 69:171-175.

16. Ahn, Y.; Lee, H.S.; Lee, S.H.; Joa, K.L.; Lim, C.Y.; Ahn, Y.J.; Hong, K.B. Effects of gypenoside L-containing *Gynostemma pentaphyllum* extract on fatigue and physical performance: A double-blind, placebo-controlled, randomized trial. *Phytotherapy Research*. 2023;37(7):3069-3082.
17. Li, Y.; Ouyang, Q.; Li, X.; Alolgal, R.N.; Fan, Y.; Sun, Y.; Ma, G. The role of *Gynostemma pentaphyllum* in regulating hyperlipidemia. *The American Journal of Chinese Medicine*. 2023;51(04):953-978.
18. Ren, D.; Zhao, Y.; Zheng, Q.; Alim, A.; Yang, X. Immunomodulatory effects of an acidic polysaccharide fraction from herbal *Gynostemma pentaphyllum* tea in RAW264. 7 cells. *Food & Function*. 2019;10(4):2186-2197.
19. Zhang, Z.; Zhang, W.; Ji, Y.P.; Zhao, Y.; Wang, C.G.; Hu, J.F. Gynostemosides A-E, megastigmane glycosides from *Gynostemma pentaphyllum*. *Phytochemistry*. 2010; 71(5-6):693-700.
20. Liu, H.L.; Kao, T.H.; Chen, B.H. Determination of carotenoids in the chinese medical herb Jiao-Gu-Lan (*Gynostemma Pentaphyllum* MAKINO) by liquid chromatography. *Chromatographia*. 2004;60(7):411-417.
21. Huang, S.C.; Hung, C.F.; Wu, W.B.; Chen, B.H. Determination of chlorophylls and their derivatives in *Gynostemma pentaphyllum* Makino by liquid chromatography-mass spectrometry. *J Pharm Biomed Anal*. 2008; 48(1):105-112.
22. Wang, X.W.; Zhang, H.P.; Chen, F.; Wang, X.; Wen, W.Y. A new lignan from *Gynostemma pentaphyllum*. *Chinese Chem Lett*. 2009; 20(5):589-591.
23. Yang, X.; Zhao, Y.; Yang, Y.; Ruan, Y. Isolation and characterization of immunostimulatory polysaccharide from an herb tea, *Gynostemma pentaphyllum* Makino. *J Agric Food Chem*. 2008;56(16):6905-6909.
24. Bai, M.S.; Gao, J.M.; Fan, C.; Yang, S.X.; Zhang, G.; Zheng, C.D. Bioactive dammarane-type triterpenoids derived from the acid hydrolysate of *Gynostemma pentaphyllum* saponins. *Food Chem*. 2010; 119(1):306-310.
25. Yan, H.; Wang, X.; Wang, Y.; Wang, P.; Xiao, Y. Antiproliferation and anti-migration induced by gypenosides in human colon cancer SW620 and esophageal cancer Eca-109 cells. *Hum Exp Toxicol*. 2014; 33(5):522-533.
26. Yin, Q.; Chen, H.; Ma, R.H.; Zhang, Y.Y.; Liu, M.M.; Thakur, K.; Wei, Z.J. Ginsenoside CK induces apoptosis of human cervical cancer HeLa cells by regulating autophagy and endoplasmic reticulum stress. *Food & Function*. 2021; 12(12): 5301-5316.
27. Tavakoli, F.; Jahanban-Esfahlan, R.; Seidi, K.; Jabbari, M.; Behzadi, R.; Pilehvar-Soltanahmadi, Y.; Zarghami, N. Effects of nano-encapsulated curcumin-chrysin on telomerase, MMPs and TIMPs gene expression in mouse B16F10 melanoma tumour model. *Artificial cells, nanomedicine, and biotechnology*. 2018; 46:75-86.
28. Van Meerloo, J.; Kaspers, G.J.L.; Cloos, J. Cell sensitivity assays: the MTT assay. *Cancer cell Cult methods Protoc*. 2011;237-245.
29. Zhang, Y.Y.; Zhang, F.; Zhang, Y.S.; Thakur, K.; Zhang, J.G.; Liu, Y.; Kan, H.; Wei, Z.J. Mechanism of juglone-induced cell cycle arrest and apoptosis in Ishikawa human endometrial cancer cells. *J Agric Food Chem*. 2019; 67(26):7378-7389.
30. Hussain, S.S.; Zhang, F.; Zhang, Y.; Thakur, K.; Naudhani, M.; Cespedes-Acuña, C.L.; Wei, Z.J. Stevenleaf from *Gynostemma pentaphyllum* inhibits human hepatoma cell (HepG2) through cell cycle arrest and apoptotic induction. *Food Sci Hum Wellnes*. 2020; 9(3):295-303.
31. Darzynkiewicz, Z. *Recent advances in cytometry*. Academic Press. 2011.
32. Petersen, R.C. Mild cognitive impairment as a diagnostic entity. *J Intern Med*. 2024;256(3):183-194.
33. Thompson, C.B. Apoptosis in the pathogenesis and treatment of disease. *Science*. 1995; 267(5203):1456-1462.
34. Leist, M.; Jäätelä, M. Four deaths and a funeral: from caspases to alternative mechanisms. *Nat Rev Mol Cell Biol*. 2001; 2(8):589-598.
35. Green, D.R.; Kroemer, G. The pathophysiology of mitochondrial cell death. *Science*. 2004;305(5684):626-629.
36. Massagué, J. G1 cell-cycle control and cancer. *Nature*. 2004;432(7015):298-306.
37. Karimian, A.; Ahmadi, Y.; Yousefi, B. Multiple functions of p21 in cell cycle, apoptosis and transcriptional regulation after DNA damage. *DNA Repair*. 2016; 42:63-71.
38. Wang, J.; Liao, A.M.; Thakur, K.; Zhang, J.G.; Huang, J.H.; Wei, Z.J. Licochalcone B extracted from *Glycyrrhiza uralensis* Fisch induces apoptotic effects in human hepatoma cell HepG2. *J Agric Food Chem*. 2019; 67(12):3341-3353.

39. Serrano, M.; Hannon, G.J.; Beach, D. A new regulatory motif in cell-cycle control causing specific inhibition of cyclin D/CDK4. *Nature*. 1993; 366(6456):704-707.
40. Ruas, M.; Peters, G. The p16INK4a/CDKN2A tumor suppressor and its relatives. *Biochim Biophys Acta (BBA)-Reviews Cancer*. 1998; 1378(2):F115-F177.
41. Fan, J.P.; Kim, H.S.; Han, G.D. Induction of apoptosis by L-carnitine through regulation of two main pathways in Hepa1c1c 7 cells. *Amino Acids*. 2009; 36:365-372.
42. McCoy, M.K.; Tansey, M.G. TNF signaling inhibition in the CNS: implications for normal brain function and neurodegenerative disease. *J Neuroinflammation*. 2008; 5:1-13.
43. Siddiqui, W.A.; Ahad, A.; Ahsan, H. The mystery of BCL2 family: Bcl-2 proteins and apoptosis: an update. *Arch Toxicol*. 2015;89:289-317.
44. Pan, Z.; Zhang, X.; Yu, P.; Chen, X.; Lu, P.; Li, M.; Li, D. Cinobufagin induces cell cycle arrest at the G2/M phase and promotes apoptosis in malignant melanoma cells. *Frontiers in Oncology*. 2019; 9:853.
45. Sun, Y.S.; Thakur, K.; Hu, F.; Zhang, J.G.; Wei, Z.J. Icariside II inhibits tumorigenesis via inhibiting AKT/Cyclin E/CDK 2 pathway and activating mitochondria-dependent pathway. *Pharmacol Res*. 2020; 152:104616.
46. Wang, J.; Zhang, Y.S.; Thakur, K.; Hussain, S.S.; Zhang, J.G.; Xiao, G.R.; Wei, Z.J. Licochalcone A from licorice root, an inhibitor of human hepatoma cell growth via induction of cell apoptosis and cell cycle arrest. *Food Chem Toxicol*. 2018;120:407-417.

**Disclaimer/Publisher's Note:** The statements, opinions and data contained in all publications are solely those of the individual author(s) and contributor(s) and not of MDPI and/or the editor(s). MDPI and/or the editor(s) disclaim responsibility for any injury to people or property resulting from any ideas, methods, instructions or products referred to in the content.